Electronic Supplementary Material (ESI) for Physical Chemistry Chemical Physics.

Trends in the Stability of Covalent Dative Bonds with Variable Solvent Polarity Depend on the Charge Transfer in the Lewis Electron-Pair System

Rabindranath Lo,[†a,b] Debashree Manna,[†a] Vijay Madhav Miriyala,[a,b] Dana Nachtigallová,[a,c] and Pavel Hobza[*a,c]

[a.] *Institute of Organic Chemistry and Biochemistry, Czech Academy of Sciences, v.v.i., Flemingovo nám. 2, 16000 Prague 6, Czech Republic.*
[b.] *Regional Centre of Advanced Technologies and Materials, Czech Advanced Technology and Research Institute, Palacký University Olomouc, Křížkovského 511/8, Olomouc 77900, Czech Republic*
[c.] *IT4Innovations, VŠB-Technical University of Ostrava, 17. listopadu 2172/15, 70800 Ostrava-Poruba, Czech Republic*
† Both authors contributed equally to this work and can be considered as the first author.
Email: pavel.hobza@uochb.cas.cz

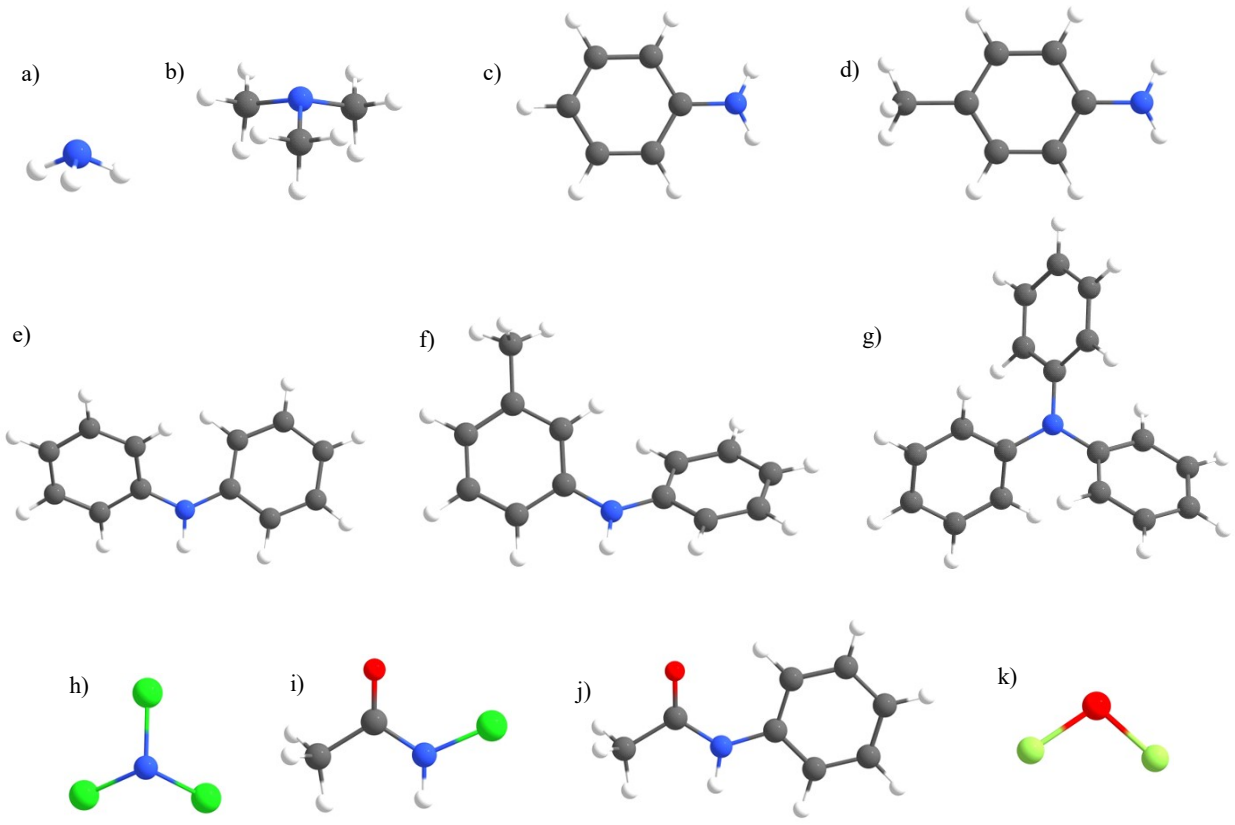

Fig. S1 The donor molecules considered in this study. a) NH_3, b) NMe_3, c) NH_2Ph, d) $NH_2Ph(4\text{-}Me)$, e) $NHPh_2$, f) $NHPhPh(3\text{-}Me)$, g) NPh_3, h) NCl_3, i) NHClCOMe, j) NHPhCOMe and k) OF_2. [C: grey, H: hydrogen, N: blue, O: red, Cl: green, F: yellowish green]

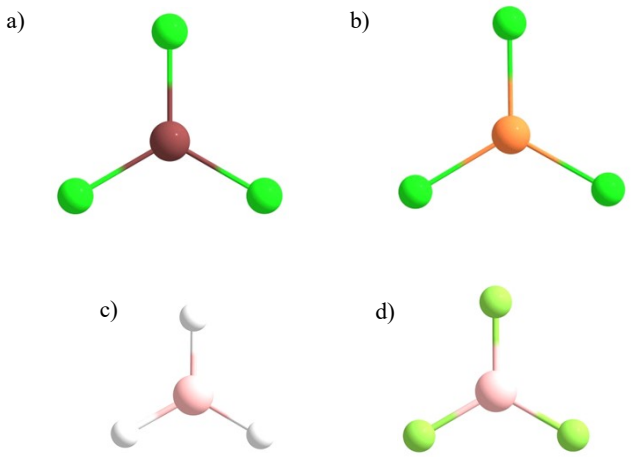

Fig. S2 The acceptor molecules considered in this study. a) $GaCl_3$, b) $InCl_3$, c) BH_3 and d) BF_3. [H: hydrogen, Cl: yellowish green, B: pink, Ga: brown, In: dark orange]

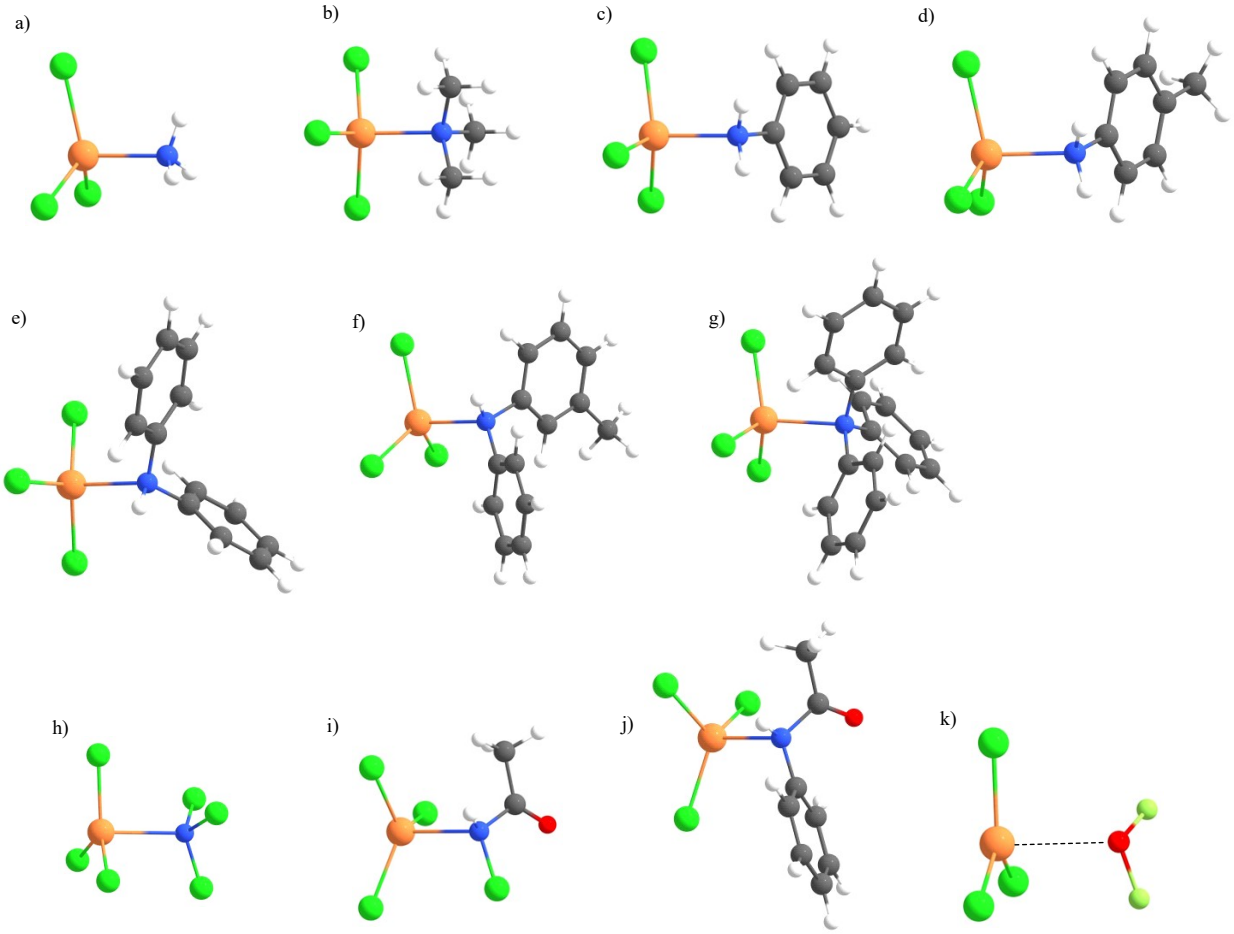

Fig. S3 The optimized geometries of $InCl_3$ complexes with various donor molecules. a) $InCl_3$-NH_3, b) $InCl_3$-NMe_3, c) $InCl_3$-NH_2Ph, d) $InCl_3$-NH_2Ph(4-Me), e) $InCl_3$-$NHPh_2$, f) $InCl_3$-NHPhPh(3-Me), g) $InCl_3$-NPh_3, h) $InCl_3$-NCl_3, i) $InCl_3$-NHClCOMe, j) $InCl_3$-NHPhCOMe and k) $InCl_3$...OF_2. [C: grey, H: hydrogen, N: blue, O: red, Cl: green, F: yellowish green, In: dark orange]

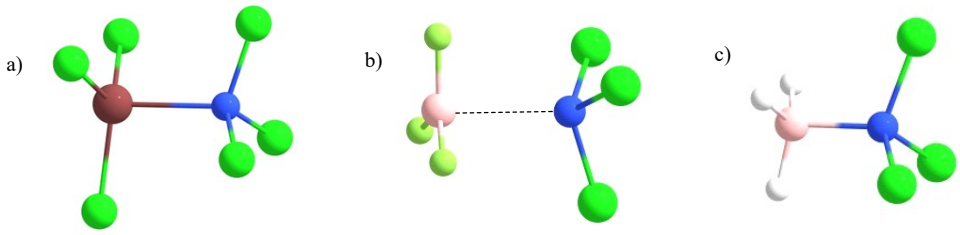

Fig. S4 The optimized geometries of NCl_3 complexes with various acceptor molecules. a) NCl_3-$GaCl_3$, b) NCl_3...BF_3 and c) NCl_3-BH_3. [H: hydrogen, Cl: yellowish green, B: pink, Ga: brown, N: blue]

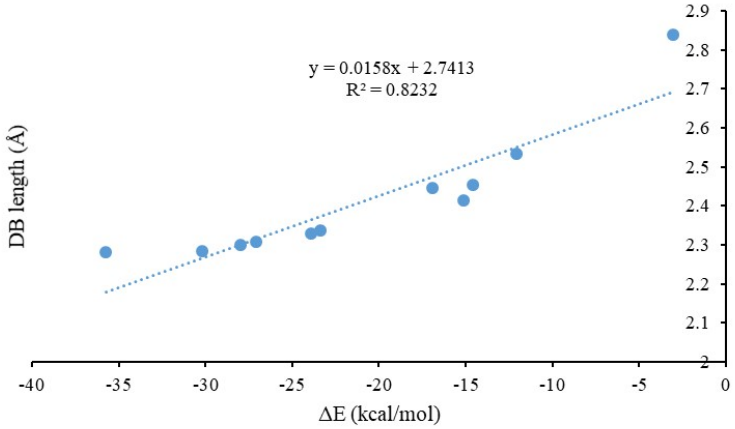

Fig. S5 The correlation of interaction energy (ΔE) with dative bond length (Å).

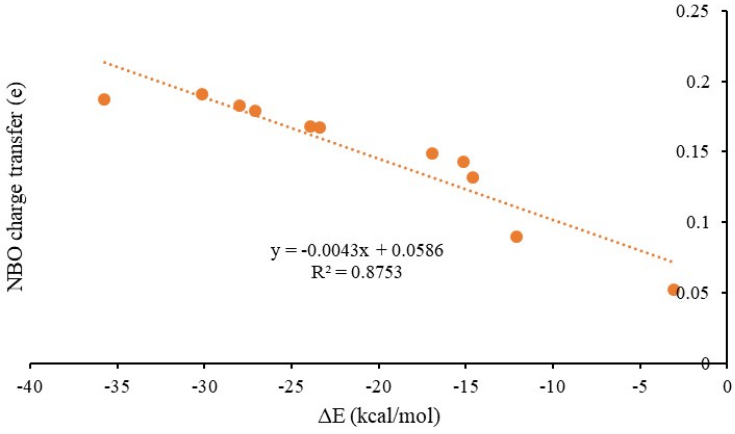

Fig. S6 The correlation of interaction energy (ΔE) with NBO charge transfer (e).

Computation

Structures of all subsystems and complexes were optimized at the DFT-D level using the PBE0-D3[1,2] functional with zero damping and def2-QZVP basis set.[3] The binding free energies (ΔG_{calc}) at 298 K were

determined using the rigid rotor–harmonic oscillator–ideal gas approximation at the same computational level.

Solvents considered were modelled with the COSMO continuous solvation model;[4] reliability of the model with respect to other continuous solvent models as well as to explicit solvent model was verified in our earlier papers.[5,6] In the present paper the COSMO model will be used only for aprotic non-donor solvents. Solvent in the continuous model is characterized by its dielectric constants ε, which ammounts to 1.0, 2.6, 4.8, 8.9 and 9.99 for the gas phase, carbon disulfide, chloroform, dichloromethane and o-dichlorobenzene (DCB), respectively. The respective solvation energy consists of electrostatic and non-electrostatic terms,

$$\Delta E_{solv} = \Delta E_{solv}\,(\text{elec}) + \Delta E_{solv}\,(\text{non-elec})\,, \qquad \text{(S1)}$$

where the latter term is formed by dispersion, H-bonding, cavity and surface contributions. The surface contribution is estimated using the solvent accesible surface area (SASA). The solvation energy of the system is calculated as a difference between the energy of the optimized system in the solvent and the energy of that geometry in the gas phase; by construction the solvation energy is negative. The change of solvation energy (ΔE_{solv}) is defined as a difference between the solvation energies of the complex and separated subsystems, respectively. A negative value of ΔE_{solv} indicates higher stabilization of the complex with respect of subsystems while its positive value indicates opposite. DB stability increase with increasing solvent polarity is connected with the negative ΔE_{solv} while the DB stability decrease with positive ΔE_{solv}.

For few complexes involving heavy elements (In, Ga) relativistic effects are incorporrated using relativistic-ZORA mostly at PBE0-D3/ZORA-def2-TZVP level. Only for In, SARC-ZORA-TZVP basis has been used. We have also used the SARC/J auxiliary basis set, which is more accurate for relativistic ZORA calculations.

Charge transfer (CT) was determined using the NBO analyses.[7] Throughout the paper the Gaussian 16 program package[8] was utilized. Mayer bond order was calculated at PBE0-D3/def2-QZVP level of theory.

The constrained DFT (cDFT) calculations[9] which eliminate the charge transfer in the Lewis electron-pair system were performed at PBE0-D3/def2-TZVPP level using NWCHEM version 7.0.2.[10] For few complexes, the cDFT calculations were performed at PBE0-D3/def2-QZVP level. The technique was applied not only for determination of total and solvation energies but also of complex dipole moments. The Löwdin charge transfer (in e) values were calculated using NWCHEM version 7.0.2.

Molecular dynamics (MD) simulations with the explicit solvent model were performed for selected systems to verify the reliability of the continuous solvent model. In particular, the MD simulations were performed for $InCl_3$—NH_3, $InCl_3$—NCl_3, $GaCl_3$-NCl_3 and BH_3—NCl_3 complexes in vacuo and embedded in a cluster of 20 molecules of carbon disulfide and 10 molecules of DCB in a cubic restraint box of 20 Å length. Molecular dynamics trajectories were simulated by ORCA 5.0.3 code[11] and visualized by VMD 1.9.2 visualization software.[12] All the simulations were performed at the PBE0-D3BJ/6-31G* level of theory. The simulation time was performed up to 10 ps for calculations involving solvents and also for gas phase. In the simulation, the step size was set to 1 fs, Nose–Hoover chain thermostat (NHC) with high-order Yoshida integrator[13,14] with time constant of 20 fs was employed to control the temperatures. The temperature for all the simulations was set at 300 K. Average distances of the central bond in respective solvents were calculated for each complexes in various solvents.

Electrostatic potential of a molecule is obtained from the formatted chk files calculated by Gaussian 16[8] at PBE0-D3/def2-QZVP level. The $V_{s,max}$ and $V_{s,min}$ values are calculated using Multiwfn 3.6 software.[15]

Results

Molecular Dynamics Simulations

The results obtained from the continuous solvent model have been verified using a more reliable explicit solvent model. The results obtained from both the models are in good agreement. $InCl_3$-NH_3 is stable in the gas and in both explicit CS_2 and DCB with In-N bond lengths of 2.297, 2.310 and 2.298 Å respectively, while $InCl_3$-NCl_3 is stable in the gas and explicit CS_2 with In-N distance of 2.466 Å and 2.568 Å, respectively but becomes weaker in explicit DCB with In-N distance of 2.697 Å. NCl_3-BH_3 on the other hand remains stable in the gas, explicit CS_2 and DCB with a B-N bond length of 1.641, 1.667 Å and 1.661 Å. The $GaCl_3$-NCl_3 complex remains stable in the gas but becomes weaker in explicit CS_2 and DCB with a Ga-N bond length of 2.186 Å, 2.261 Å and 2.404 Å, respectively. Plots of the trajectories ~ 10 ps for all the complexes in the gas, CS_2 and DCB are given below (Figs. S7-S10). It can be seen that $InCl_3$-NH_3 and BH_3-NCl_3 complexes are stabilized in the gas, CS_2 and DCB, while $InCl_3$-NCl_3 and $GaCl_3$-NCl_3 become weaker upon passing from CS_2 and DCB.

Table S1 Interaction energy (ΔE), binding free energy (ΔG) (in kcal/mol, T = 298 K) of various DB complexes in different solvents calculated at PBE0-D3/ZORA-def2-TZVP level of theory using relativistic ZORA approach.

Complex	ΔG	ΔE
$InCl_3$…NH_3		
Gas	-16.87	-29.41
CS_2	-19.03	-31.83
Chloroform	-19.35	-32.32
DCM	-21.44	-34.47
DCB	-21.61	-34.64
$InCl_3$...NCl_3		
Gas	5.32	-8.55
CS_2	6.15	-7.71
Chloroform	7.24	-6.63
DCM	6.76	-7.07
DCB	6.79	-7.04
$GaCl_3$...NCl_3		
Gas	5.77	-8.43
CS_2	5.94	-8.37
Chloroform	6.06	-8.30
DCM	5.97	-8.41
DCB	5.96	-8.42

Table S2 Interaction energy (ΔE), binding free energy (ΔG) (in kcal/mol, T = 298 K) of various DB complexes in different solvents calculated at MP2/def2-TZVP level of theory.

Complex	ΔG	ΔE
$InCl_3$… NH_2Ph(4-Me)		
Gas	-20.78	-33.30
CS_2	-21.51	-34.47
DCB	-22.96	-35.70
$InCl_3$…NHPh2		
Gas	-18.97	-32.82
CS_2	-18.63	-32.71
DCB	-18.54	-32.83
$InCl_3$…NHPhPh(3-Me)		
Gas	-19.68	-33.50
CS_2	-19.12	-33.33
DCB	-18.76	-33.47

Table S3 Mayer bond order of complexes in various solvents.

Complex	Mayer bond order
$InCl_3$…NH_3	
Gas	0.357
CS_2	0.441
Chloroform	0.494
DCM	0.498
DCB	0.502
$InCl_3$...NCl_3	
Gas	0.234
CS_2	0.249
Chloroform	0.255
DCM	0.259
DCB	0.260
$GaCl_3$...NCl_3	
Gas	0.292
CS_2	0.319
Chloroform	0.329
DCM	0.336
DCB	0.336

Table S4 NBO Charge transfer (in e) of complexes with explicit solvent molecules calculated at PBE0-D3/def2tzvpp.

Complex	CT
$InCl_3$...NH_3	
Gas	0.169
CS_2	0.17
DCB	0.173
$InCl_3$...NCl_3	
Gas	0.08
CS_2	0.126
DCB	0.128
BH_3...NCl_3	
Gas	0.202
CS_2	0.238
DCB	0.243
$GaCl_3$...NCl_3	
Gas	0.104
CS_2	0.113
DCB	0.124

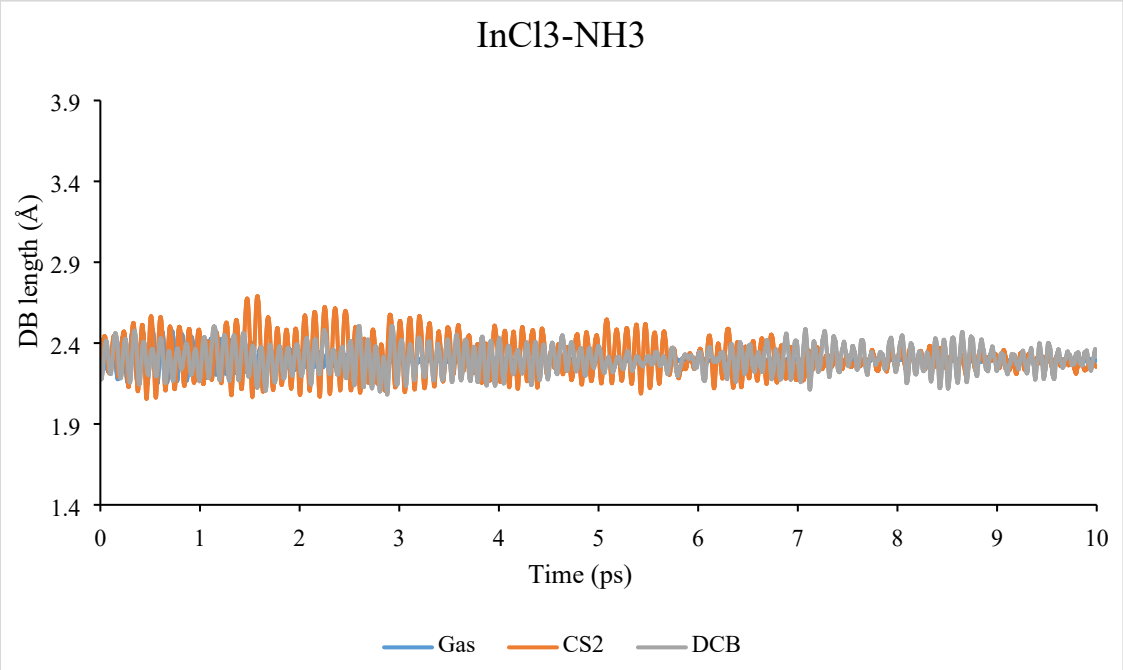

Fig. S7 Molecular dynamics simulations of $InCl_3$-NH_3 complex in various medium at 300K.

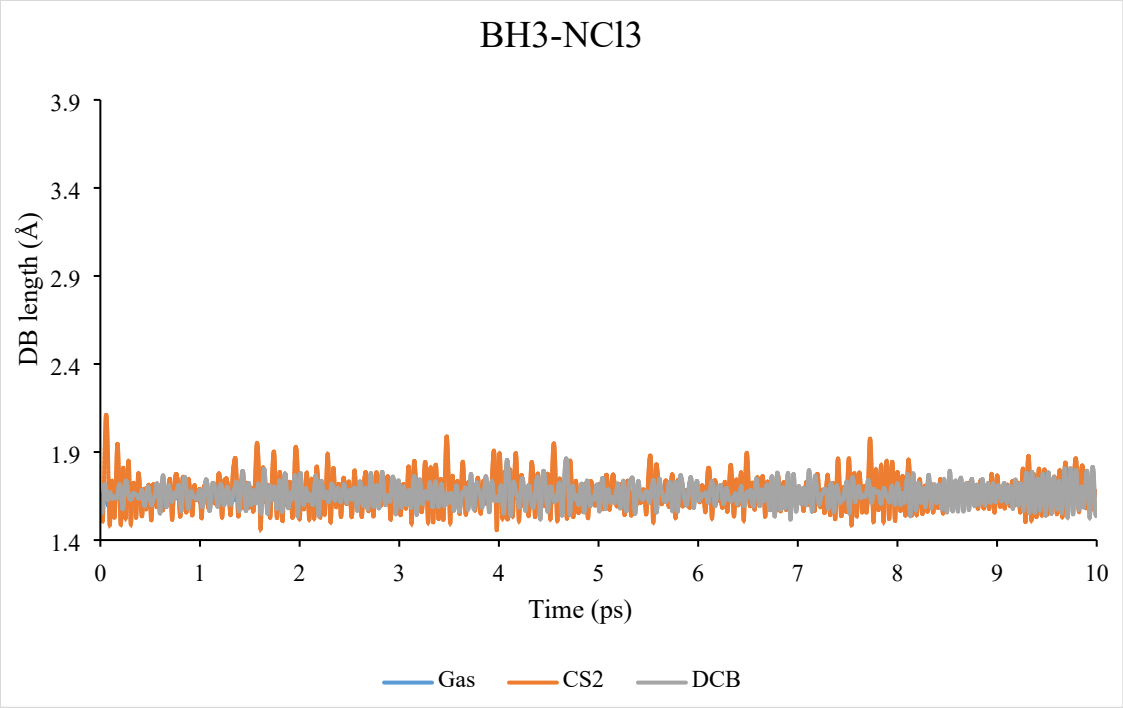

Fig. S8 Molecular dynamics simulations of BH_3-NCl_3 complex in various medium at 300K.

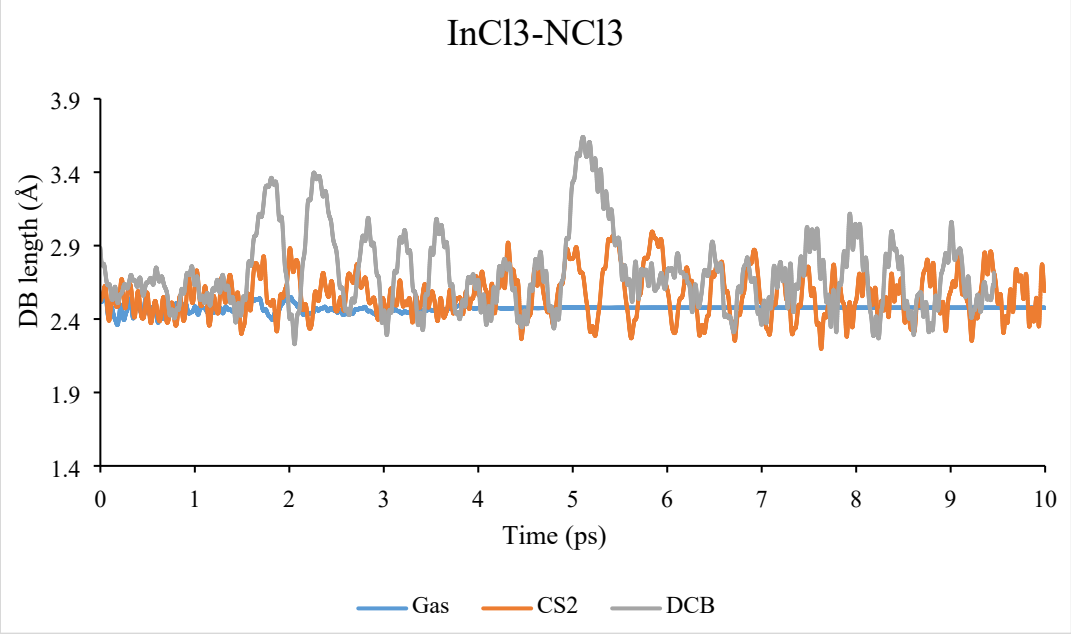

Fig. S9 Molecular dynamics simulations of $InCl_3$-NCl_3 complex in various medium at 300K.

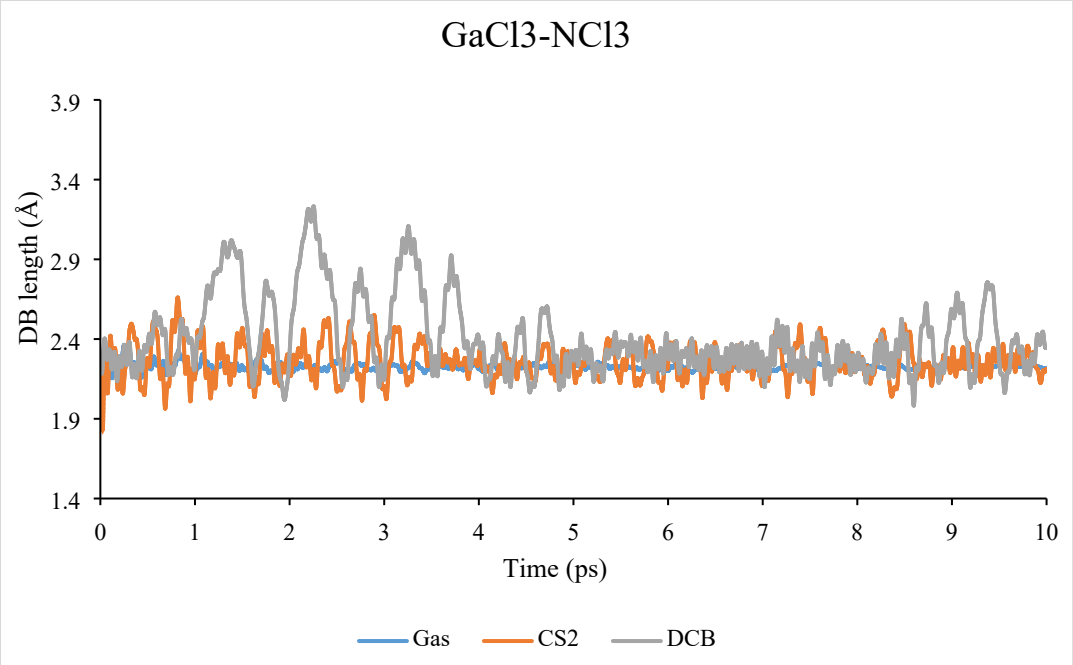

Fig. S10 Molecular dynamics simulations of $GaCl_3$-NCl_3 complex in various medium at 300K.

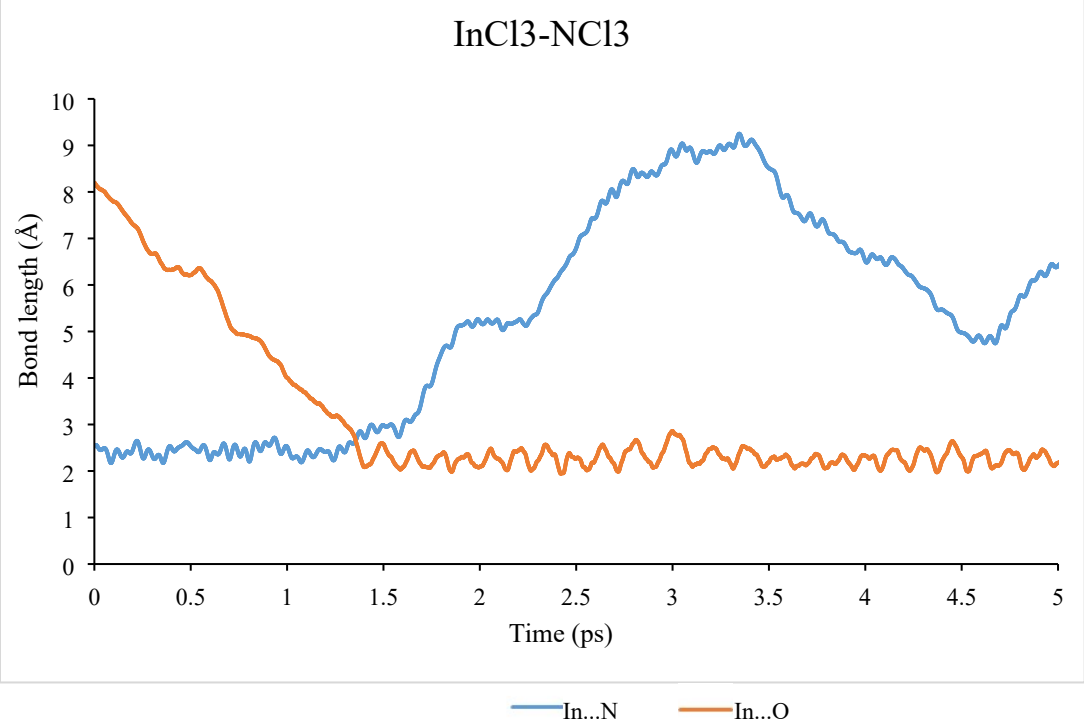

Fig. S11 Molecular dynamics simulations of $InCl_3$-NCl_3 complex in acetone medium at 300K.

References

1. C. Adamo and V. Barone, *J. Chem. Phys.*, 1999, **110**, 6158.

2. S. Grimme, J. Antony, S. Ehrlich and H. Krieg, *J. Chem. Phys*., 2010, **132**, 154104.
3. F. Weigend, *J. Comput. Chem*., 2008, **29**, 167.
4. A. Klamt and G. Schurmann, *J. Chem. Soc., Perkin Trans.,* 1993, **2**, 799.
5. V. M. Miriyala, R. Lo, P. Bouř, T. Wu, D. Nachtigallová and P. Hobza, *J. Phys. Chem. A,* 2022, **126**, 7938–7943.
6. R. Lo, D. Manna, M. Lamanec, M. Dračínský, P. Bouř, T. Wu, G. Bastien, J. Kaleta, V. M. Miriyala, V. Špirko, A. Mašínová, D. Nachtigallová and P. Hobza, *Nat. Commun*., 2022, **13**, 2107.
7. A. E. Reed, L. A. Curtiss and F. Weinhold, *Chem. Rev*., 1988, **88**, 899.
8. Gaussian 16, Revision A.03, M. J. Frisch, G. W. Trucks, H. B. Schlegel, G. E. Scuseria, M. A. Robb, J. R. Cheeseman, G. Scalmani, V. Barone, G. A. Petersson, H. Nakatsuji, et al. Gaussian, Inc.Wallingford, CT, **2016**.
9. B. Kaduk, T. Kowalczyk and T. Van Voorhis, *Chem. Rev*., 2012, **112**, 321 and references therein.
10. E. Apra, E. J. Bylaska, W. A. De Jong, N. Govind, K. Kowalski, T. P. Straatsma, M. Valiev, H. van Dam, Y. Alexeev, J. Anchell, et al. *J. Chem. Phys.*, 2020, **152**, 184102.
11. F. Neese, *WIREs Comput Mol Sci.* 2022, **12**, e1606.
12. W. Humphrey, A. Dalke and K. Schulten, *J. Mol. Graph*., 1996, **14**, 33.
13. G. J. Martyna, M. L. Klein, M. Tuckerman, *J. Chem. Phys*., 1992, **97**, 2635.
14. G. J. Martyna, M. E. Tuckerman, D. J. Tobias, M. L. Klein, Mol. Phys., 1996, **87**, 1117.
15. T. Lu, F. Chen, Multiwfn: A Multifunctional Wavefunction Analyzer. *J. Comput. Chem.* 2012, ***33* (5)**, 580.